Journal of Research in Mechanics of Agricultural Machinery/Vol. 15 /No.2 /Serial No. 39/ Summer 2026

Journal of Research in Mechanics of Agricultural Machinery

Shahrekord University

Research Paper

Numerical Simulation of a Nano-PCM Integrated PV/T Collector for Enhanced Thermal Regulation and Uniform Heat Distribution

Mohadeseh Ahmadi[1], Akbar Arabhosseini[1*], Hadi Samimi-Akhijahani [2]

[1.] Department of Agrotechnology, Faculty of Agricultural Technology (Aburaihan), University of Tehran, Tehran, Iran.

[2.] Department of Biosystem Engineering, Faculty of Agriculture, University of Kurdistan, Kurdistan, Iran.

Article History

Submited: 2026/02/23

Revised: 2026/05/22

Accepted: 2026/06/03

Published online: 2026/06/22

Keywords:

Charging and discharging

Photovoltaic panel

Thermal energy storage material

Nano-PCM

Dynamic heat transfer analysis

***Corresponding author email:**

ahosseini@ut.ac.ir

ORCID:

0000-00025572-7798

Abstract

This study presents a hybrid photovoltaic/thermal (PV/T) collector incorporating nano-enhanced phase change material (nano-PCM) for simultaneous cooling and thermal energy storage. Copper tubes filled with paraffin doped with 3 %wt. zirconium oxide(ZrO_2) nanoparticles were vertically embedded beneath the PV panel in a novel energy storage configuration to enhance heat dissipation, improve thermal uniformity, and optimize latent heat storage within the collector structure. Transient numerical simulations were conducted using CFD to analyze both charging and discharging phases of the thermal storage system. During the charging process, the nano-PCM absorbed excess solar heat, effectively stabilizing the thermal field and maintaining tube temperatures within 316–322K, while limiting the peak collector temperature to 372–389K and preventing localized thermal hotspots. In the discharging phase, the controlled release of stored latent heat sustained tube temperatures between 312–325K, maintained the central collector surface temperature at 340–345K, and kept the PV panel temperature within 300–304K, thereby ensuring stable operational thermal conditions. The proposed system introduces a novel configuration for thermal energy storage integration, enabling improved heat management, enhanced energy recovery, and prolonged system stability. Results indicate that combining nano-PCM storage with an optimized PV/T structural arrangement effectively balances heat absorption, storage, and controlled release. This approach is particularly suitable for solar drying applications, where a continuous and stable thermal energy supply is essential for maintaining product quality and process efficiency.

How to cite this paper:

Ahmadi, M., Arabhosseini, A., and Samimi-Akhijahani, H. (2026). Numerical Simulation of a Nano-PCM Integrated PV/T Collector for Enhanced Thermal Regulation and Uniform Heat Distribution. *Journal of Research in Mechanics of Agricultural Machinery*. 39: 29-40. https://dx.doi.org/10.22034/jrmam.2026.14951.758.

https://dx.doi.org/10.22034/jrmam.2026.14951.758

1. Introduction

Global population growth and technological advancement have significantly increased demand for fossil fuels worldwide. However, these resources are finite, and their extensive use has led to serious environmental problems, particularly the emission of greenhouse gases that contribute to global warming and climate change. These challenges have prompted many countries to shift toward renewable energy sources in pursuit of energy security and environmental protection (Makieła et al., 2022). Renewable energy sources are natural resources that provide energy and are replenished continuously or at a rate faster than their consumption within a reasonable timeframe. These sources are recognized as sustainable and low-risk alternatives to fossil fuels. Although fossil fuels are natural resources, their extremely slow regeneration rate makes them effectively non-renewable. Furthermore, their use releases carbon dioxide, which significantly contributes to the greenhouse effect and global warming (Boyle & Redgwell., 2021).

The main types of renewable energy sources include solar, wind, geothermal, biomass, tidal, wave, and hydropower (Koohi-Fayegh & Rosen., 2020). Despite the high potential and promising characteristics of renewable energy sources, particularly solar and wind energy, exhibit inherent variability and intermittency. This instability is primarily due to their dependence on time- and weather-dependent conditions, such as solar irradiance levels or wind speed. Therefore, to ensure a reliable and stable energy supply, it is essential to integrate these resources with other renewable energy sources or suitable energy storage systems (Nair et al., 2022; Rezk et al., 2021).

Furthermore, global projections indicate that the share of renewable energy sources in electricity generation will exceed 80% in the near future, leading to a significantly increased demand for high-capacity, cost-effective, and operationally flexible energy storage systems within power networks (Kaushik et al., 2022). Solar energy, originating from the Sun, a massive celestial body with a diameter of approximately 1.39×10^9 meters located at an average distance of 1.5×10^{11} meters from Earth constitutes the primary source of energy on Earth (Singh et al., 2021). The Sun delivers an approximate irradiance of 1366 W/m^2 to the upper layers of the Earth's atmosphere. The annual solar energy reaching the Earth’s surface is estimated at about 5.46×1024 joules, which exceeds the current global energy demand by more than 10,000 times (Hossain, 2021).

This abundant availability of clean, renewable energy has positioned solar power as one of the most crucial energy resources for meeting future global energy needs while significantly mitigating environmental concerns associated with fossil fuel consumption (El-Afifi., 2024). Solar energy can be utilized in various agricultural applications, including drying agricultural products, heating greenhouses and livestock facilities, and supplying energy for water pumps, ventilation systems, etc. (Arabhosseini, 2023). The solar technologies employed in this field generally include thermal and electrical systems, among which photovoltaic panels, solar water heaters, solar desalination units, and solar dryers are the most prominent (Khoja., 2022). Drying agricultural products is an efficient and affordable method for processing and preventing spoilage.

Solar dryers, by harnessing renewable solar energy, provide a practical, economical, and environmentally friendly solution for drying food products. Indirect solar dryers use solar radiation to dry food products in a closed and hygienic environment. Unlike traditional methods, which expose food to dust, insects, and contamination in open air, this approach reduces contamination risk and helps preserve product quality. Compared to industrial dryers, indirect solar dryers offer significant advantages, including lower energy consumption, reduced costs, and no emissions of harmful gases. Despite the numerous advantages of solar dryers, these systems have certain limitations, such as interruptions in the drying process under unfavorable weather conditions, including dense cloud cover, rainfall, and the absence of sunlight at night. To overcome these challenges and ensure continuous operation of the drying process under all environmental conditions, various methods have been employed, notably thermal energy storage systems to provide the necessary heat. This approach helps prevent product damage and maintains its quality (Kumar et al., 2023). Figure 1 schematically illustrates the phase change process.

During phase transition, such as melting (solid to liquid) or solidification (liquid to solid), a material absorbs or releases substantial thermal energy while maintaining an approximately constant temperature. This characteristic classifies phase change materials (PCMs) as latent heat storage (LHS) media. PCMs effectively balance energy supply and demand by storing surplus thermal energy during periods of high solar irradiance and releasing it during low-irradiance intervals or nighttime, thereby minimizing energy waste and ensuring continuous thermal availability for applications such as solar drying (Zhou et al., 2019).

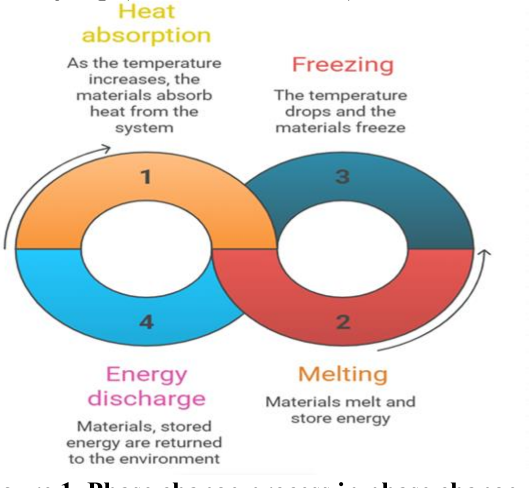

Figure 1. Phase change process in phase change materials

Since the collector is the most critical component of a solar drying system, its thermal performance and optimal design play a significant role in the overall system efficiency and the quality of the drying process. Optimizing the collector structure, selecting appropriate materials, and employing modern techniques can improve energy efficiency, reduce heat losses, and enhance the uniformity of the drying process under varying environmental conditions. Photovoltaic/Thermal (PV/T) systems are hybrid solar technologies that simultaneously convert solar radiation into both electrical and thermal energy. By reducing the temperature of the photovoltaic (PV) module, these systems improve its electrical efficiency while also delivering substantial thermal energy.

A typical PV/T system consists of a PV module, a thermal absorber, and a cooling fluid. Compared to the separate use of a flat-plate thermal collector and a PV panel, PV/T systems can generate up to 230% more power (Lämmle et al., 2017). The use of nanofluids as cooling agents significantly improves both thermal and electrical performance due to their superior thermal conductivity (Abdelrazik et al., 2018). In a numerical study using ANSYS Fluent, the effects of incorporating Al_2O_3, CuO, and graphene nanoparticles into paraffin wax as a nano-enhanced phase change material (NePCM) were investigated to assess their impact on thermal energy storage (TES) performance. The results showed that although increasing nanoparticle concentration increased viscosity, the enhanced thermal conductivity and reduced latent heat offset these negative effects, resulting in improved energy storage efficiency. Specifically, the addition of 0.5% Al_2O_3 led to a 4.975% increase in efficiency, while 3% graphene yielded up to a 7.118% improvement. The CuO nanoparticles also demonstrated a significant positive impact on thermal performance. These findings confirm the high potential of nano-PCMs for improving TES systems (Nandi & Biswas., 2025).

In a study, two PV/T air collectors with latent heat storage units were developed: one containing pure paraffin and the other containing paraffin combined with 1 %wt aluminum oxide (Al_2O_3) nanoparticles. The addition of nanoparticles reduced the drying time by approximately 15–22%.

Furthermore, the system's energy efficiency increased by approximately 6.97%, and its exergy efficiency improved by approximately 9.47%. The combination of nanoparticle integration and increased airflow rate resulted in a 28.58% enhancement in exergy efficiency (Sirin al., 2023). A new PV/T system was designed and numerically analyzed, comprising an aerogel layer, a phase change material (PCM), and active cooling. In this system, a silica aerogel layer with very low thermal conductivity (0.02 W/m.K) and high spectral transmittance was placed on top of the PV panel to reduce radiative and convective heat losses. Beneath the panel, a PCM chamber filled with $CaCl_2.H_2O$ mixed with expanded graphite (EG) was installed to improve thermal conductivity.

Helical active cooling pipes embedded within this layer played a key role in enhancing charging and discharging rates. Simulations performed using ANSYS Fluent showed that this design could increase energy and exergy efficiency by over 40% in summer and 42% in winter. Additionally, significant reductions in CO_2 emissions and favorable return on investment were reported. These results demonstrate the high potential of this structure to improve the thermo-electric performance of solar systems (Zheng & Zhou., 2023).

Among various metal oxides, zirconium oxide (ZrO_2) nanoparticles offers specific advantages. As reported in the literature, ZrO_2 enhances the thermal conductivity of PCM, improves the efficiency and thermal performance of thermal energy storage systems, and is applicable in thermochemical energy storage devices (Mishra et al., 2025). Regarding the selection of 3%wt concentration, most previous studies, such as Mahdi et al., (2024), investigated the range of 2–4 %wt as the optimal concentration for oxide nanoparticles. Therefore, in the present study, 3% was chosen as the average value within this range.

Therefore, in this study, a photovoltaic/thermal (PV/T) collector with a novel design was developed and analyzed using computational fluid dynamics (CFD). The primary innovation of this research lies in the development of a new nanocomposite phase change material (nanoPCM) composed of paraffin enhanced with 3% wt zirconium oxide (ZrO_2) nanoparticles. According to the authors' literature review, this specific combination has not been previously used in PV/T systems for thermal energy storage and panel cooling.

Moreover, the system features a unique geometric configuration in which copper tubes filled with the nanoPCM are vertically embedded at the bottom of the collector surface, with the photovoltaic panel mounted directly above them. It is suggested that this arrangement improves heat absorption, enhances the PV panel's cooling efficiency, and enables more effective thermal storage integration, particularly beneficial in solar drying applications. This combined material and structural innovation offers a new pathway for advancing high-efficiency PV/T-PCM collector systems.

2. Materials and Methods

2.1. PV/T Collector System and Physical Structure

In this study, a hybrid photovoltaic/thermal (PV/T) flat-plate solar collector was designed and developed to optimize thermal performance and reduce the solar panel's surface temperature. This hybrid system was designed to generate electrical energy from the photovoltaic panel and to absorb and remove excess heat using PCMs and airflow, thereby increasing the system's thermal energy. The collector structure, as shown in Figure 2, consists of a flat-plate photovoltaic solar panel, a thermal absorber plate made of galvanized steel with high thermal conductivity, coated in matte black to maximize solar radiation absorption, and a set of 25 vertically arranged copper tubes mounted behind the panel.

The tubes are vertically arranged inside the collector. These tubes are filled with nano-PCM composed of paraffin and zirconium oxide (ZrO_2) nanoparticles. In this vertical arrangement, direct contact between the tube lateral surfaces and the absorber plate is avoided. In contrast, horizontal tube placement would result in direct contact with the absorber surface, leading to localized overheating, potential PCM leakage, and non-uniform temperature distribution. Moreover, the vertical orientation facilitates natural convection within the molten PCM, resulting in more uniform melting and solidification, thereby improving the overall thermal performance of the system.

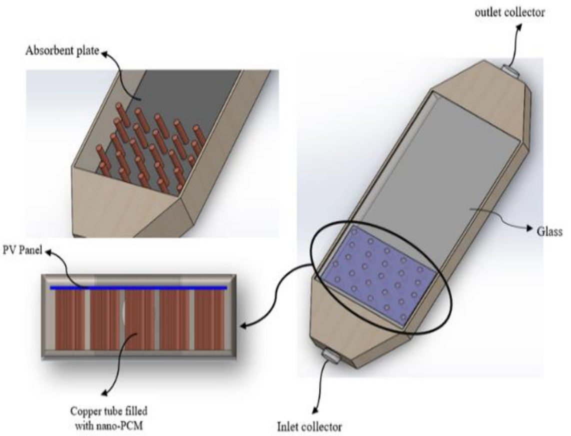

Figure 2. Schematic diagram of the solar collector

Additionally, an electric fan was installed at the collector inlet to control airflow velocity. Heat transfer in this system occurs in two ways: first, solar radiation hits the PV panel and generates electrical energy; second, the heat produced by radiation absorption in the panel and the absorber plate is transferred to the tubes containing the PCM. Forced air flow, passing through the space between the tubes, cools the tubes as well as the panel surface and increases the collector efficiency, and its schematic is shown in Figure 3.

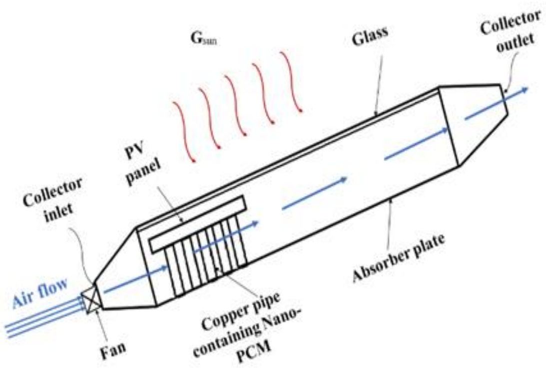

Figure 3. Schematic diagram of air flow path and thermal processes inside the collector.

This design is particularly suitable for solar drying applications, where precise temperature control is important. Based on this design, the present study provides the foundation for thermal and fluid flow simulations, and the collector configuration has been prepared for numerical analysis in the ANSYS Fluent software environment.

Figure 4 illustrates the steps followed in the numerical simulation process of the PV-T collector system. This diagram outlines the main stages of the work, from geometric design and mesh generation to thermal performance evaluation using ANSYS Fluent. Each step is clearly shown to provide a better understanding of the simulation process. More details on each of these steps in the numerical modeling procedure are presented in the following sections.

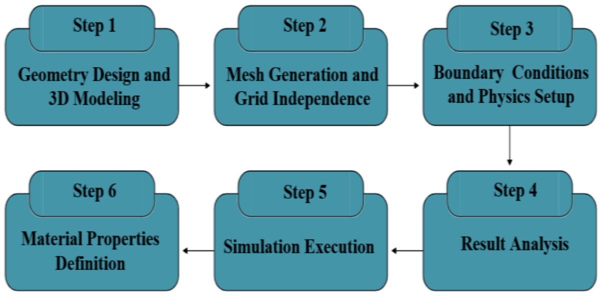

Figure 4. Numerical simulation flowchart of the PV-T system

2.2. Geometric Design and Mesh Generation

A three-dimensional model of the solar collector was developed using SolidWorks 2020. The collector dimensions were set to 180 cm (length) × 90 cm (width) × 20 cm (height), and 25 copper tubes with an outer diameter of 2 cm and a length of 17 cm were mounted vertically and uniformly behind the PV panel. The tube arrangement was designed to avoid overlap and ensure uniform airflow between them, thereby ensuring optimal heat transfer. After completing the geometry, the model was exported in x-t format and imported into ANSYS Fluent, where the mesh was generated. A combination of structured and unstructured meshes was employed: structured for geometrically simple regions and unstructured for more complex areas. To enhance simulation accuracy, the mesh was significantly refined around the tubes, at the contact area between the panel and the absorber plate, and in the thin boundary layers. Three different mesh densities (fine, medium, and coarse) were considered for the melting process.

The mesh near the PCM tubes, the solar panel, and the absorber surface was refined to better capture thermal gradients. To ensure mesh independence, the outlet air temperature from the collector was used as the evaluation criterion, confirming that the simulation results were not affected by the mesh resolution. The total number of elements for the coarse, medium, and fine meshes were approximately 1,800,000; 2,700,000; and 4,600,000 cells, respectively. Considering model accuracy, computational time, and cost efficiency, the medium mesh was selected for the simulations. A sample of the generated mesh for the collector, the PCM-filled tubes, and the PV panel is shown in Figure 5.

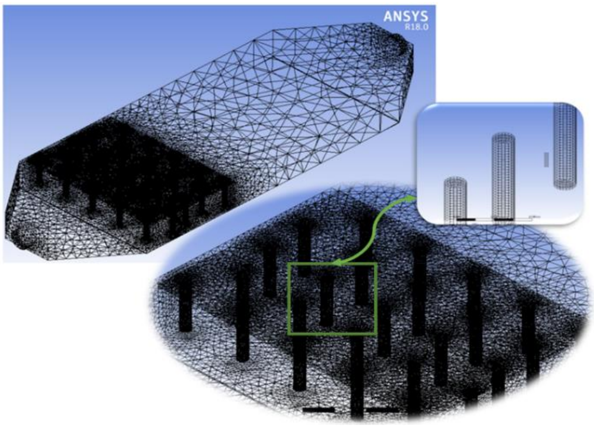

Figure 5. Mesh configuration of the solar collector system

The skewness criterion was used to evaluate the quality of the mesh employed in the simulation. For the meshing process of a system, the best and worst meshes correspond to skewness values of 0 and 1, respectively (Ahmadi et al., 2023). For the collector in this study, the fine-mesh option was selected, with a skewness value of 0.342. Moreover, as previously mentioned, the mesh independence test was performed based on the outlet temperature of the collector, and the results confirmed that the fine mesh was appropriate for the modeling process. Table 1 presents additional mesh characteristics for the collector, including element size and mesh metric parameters.

Table 1. Mesh characteristics generated for the dryer with integrated heat exchanger system.

Parameter	Value / Description	Parameter	Value / Description
Mesh type	Medium	Maximum angle	140°
Minimum size	0.0001 m	Pinch tolerance	0.0012
Maximum size	0.01 m	Inflation algorithm	Pre
Number of nodes	2,259,455	Mesh metric	Skewness
Number of elements	2,745,162	Skewness value	0.11255
Minimum angle	18.2°	-	-

2.3. Boundary Conditions and Operating Parameters

The boundary conditions defined for the simulation are as follows: Inlet Airflow: Ambient air enters the inlet section of the collector at a velocity of 1 m/s. The inlet temperature was set to 26°C (at 9:00 a.m.) for charging and 27°C (at 7:00 p.m.) for discharging. Walls: The collector's side walls are assumed to be perfectly insulated to prevent heat loss to the surroundings. The wall thickness was considered to be 0.02 m with a thermal conductivity of 0.03 W/m·K. Geographical Location: The simulation was performed for the geographical coordinates of Sanandaj city (center of Kurdistan province), with a latitude of 35.31° and a longitude of 45.99°, at an altitude of about 1530 m above sea level, during the month of August. Radiation Model: To solve the radiative heat transfer equation within each cell under a homogeneous phase, the standard DO1 (Discrete Ordinates) in ANSYS Fluent was used (Ahmadi et al., 2025). Outlet: Atmospheric pressure was applied as the outlet boundary condition to allow unobstructed airflow exit from the system.

2.4. Material properties definition

The thermophysical properties of the nano-PCM used in this research for simulation are presented in Table 2.

Table 2. Thermophysical properties of the nano-PCM used in the simulation.

Property		Value
Density (ρ)	(kg/m³)	954
Specific Heat (Cp)	(kJ/kg·K)	2.05
Thermal Conductivity	(W/m·K)	22.02
Latent Heat	(kJ/kg)	805
Melting Point	(°C)	37
Viscosity	(m²/s)	1.35×10^{-5}

Following mesh generation and grid independence verification, the thermophysical properties of the system's constituent materials were defined. The computational domain comprises six primary components: air (working fluid), copper (tubes), glass (cover), wood (insulation), galvanized sheet. The key thermophysical properties of each material are presented in Table 3.

Table 3. Characteristics of materials used in the system.

Material	Specific Heat (Cp) (J/kg·K)	Density (ρ) (kg/m³)	Thermal Conductivity (W/m·K)
Air	1006.4	1.255	0.0242
Glass	840	2579	0.96
Wood	2310	700	0.173
Copper	385	8960	401
Iron sheet	450	7874	89

2.5. Theoretical model

In general, three fundamental equations are considered for modeling a thermal system such as a solar collector with PCM. To simulate the thermal behavior of the proposed PV/T collector, the governing equations for mass, momentum, and energy conservation are solved for the airflow region.

The continuity, momentum, and energy equations are calculated using Equations (1), (2), and (3), respectively.

Continuity equation:

$$\nabla.\vec{V} = 0 \qquad (1)$$

momentum equation:

$$\rho\frac{\partial\vec{V}}{\partial t} + \rho.\vec{V}.\nabla\vec{V} = -\nabla P + \mu\nabla^2\vec{V} + \beta\vec{g}\,(T - T_{ref}) + \vec{S} \qquad (2)$$

Thermal Energy Equation:

$$\rho c_p\left(\frac{\partial h}{\partial t} + \frac{\partial H}{\partial t} + \nabla.\left(\vec{V}h\right)\right) = \nabla.(k.\nabla h) \qquad (3)$$

Which, ρ: density (kg/m³), h: specific enthalpy (J/kg), t: time (s), $\vec{V}$: the velocity vector (m/s), k: thermal conductivity (W/m.K), T: temperature (K), and C_p: Specific Heat Capacity at Constant Pressure (J/kg.K).

Given that the properties of the material cause the phase change process to affect the convection phenomenon, the source term called $\vec{S}$ is applied in Eq. 2, which can be calculated through Eq. 4:

$$\vec{S} = \frac{(1-\xi)^2}{\xi^3} A_{mush}\vec{V} \qquad (4)$$

A_{mush} is the mushy zone for PCM, generally ranging from 10^4 to 10^7 (Tay et al., 2012), and in this study it was set at 10^5.

In the case of phase change materials, the reference enthalpy is set to zero for the solid state and 1 for the liquid state. During the calculation process, the phase change of the material, which is determined by the parameter ξ (indicating the liquid fraction of paraffin) and calculated based on the temperature of the phase change material and using Eq. 5, must be taken into account:

$$\xi = \begin{cases} 0 & \text{if } T_{pcm} < T_s \\ 1 & \text{if } T_{pcm} > T_L \\ \dfrac{T - T_s}{T_s - T_s} & \text{if } T_L > T_{pcm} \end{cases} \qquad (5)$$

Total thermal capacity:

To calculate the total thermal storage capacity of the 25 tubes filled with nano-PCM, the following step-by-step procedure is used. The total stored energy consists of sensible heat and latent heat. The total thermal storage capacity for the 25 tubes filled with nano-PCM is calculated to be 246 kJ, obtained as follows:

Total volume of 25 tubes (6):

$$V_{total} = 25 \times \pi r^2 L \quad (6)$$

Total mass of nano-PCM:

$$m_{total} = \rho_{nano-PCM} \times V_{total} \quad (7)$$

Specific heat capacity of nano-PCM:

$$C_{p,nano-PCM} = (1-\phi)C_{p,PCM} + \phi C_{p,zro2} \quad (8)$$

Latent heat storage:

$$Q_{latent} = m_{total} \times L_{f,nano-PCM} \quad (9)$$

Sensible heat storage:

$$Q_{sensible} = m_{total} \times C_{p,nano-PCM} \times \Delta T \quad (10)$$

Total thermal storage capacity:

$$Q_{total} = Q_{sensible} + Q_{latent} \quad (11)$$

3. Results and Discussion

This section presents the thermal and fluid simulation results for the solar collector during charging and discharging modes of the Nano-PCM, using ANSYS Fluent.

3.1. Model Validation

To validate the present numerical model, the simulation results for pure paraffin (without nanoparticles and without PV panel) were compared with the experimental data from our previous work (Ahmadi et al., 2023). In that previous study, both experimental measurements and numerical simulations were performed for a similar collector containing pure paraffin.

Figure 6 compares the experimental data with the numerical results from the previous study for the temperature distribution during charging. The close agreement between the two sets of results confirms the accuracy of the numerical modeling approach used in that study.

In this study, the same numerical approach was extended by adding the PV panel and replacing pure paraffin with nano-PCM (paraffin with 3% ZrO_2 nanoparticles). The geometry, mesh, and solver settings remained consistent with the validated model. Therefore, the validated numerical model provides a reliable basis for investigating the thermal performance of the PV/T collector with nano-PCM. Due to current circumstances, conducting additional experiments for the new configuration (with PV panel and nano-PCM) is not possible at this time.

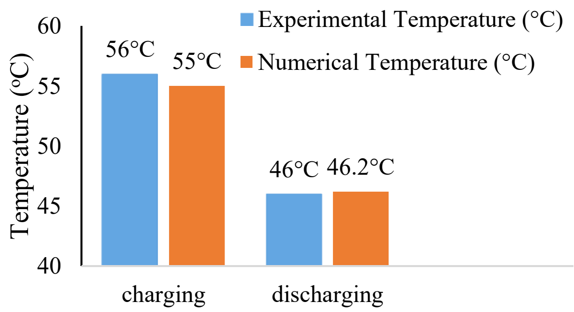

Figure 6. Validation of the numerical model: comparison of experimental and numerical outlet temperatures for pure paraffin.

3.1. Charging Mode

The Nano-PCM charging process begins early in the morning, around 8:00 AM. However, the peak heat absorption takes place during the period of maximum solar intensity, specifically from 11:00 AM to 1:00 PM. During this time, the storage medium captures surplus thermal energy and stores it as latent heat. Figure 7 illustrates the simulated temperature distribution within the collector system containing PV panels and Nano-PCM-filled tubes. At the entry point, the air temperature matches the ambient conditions. The Nano-PCM draws heat away from the PV panel, triggering its phase transition from solid to liquid. This melting phenomenon provides a cooling effect for the PV panel. As shown in the figure, the tube surfaces maintain temperatures between 316 and 322 K, represented by the blue and green zones. These values exceed the inlet air temperature, confirming successful heat absorption by the Nano-PCM. Examining the tube cross-sections reveals a distinct thermal gradient: the material closest to the tube walls undergoes melting first, while the central portion remains solid.

This pattern demonstrates that conduction is the primary heat transfer mechanism at work. The highest thermal energy accumulation occurs in the central collector areas surrounding the tubes, depicted in red and orange, with temperatures reaching 372-389 K. Moving toward the outlet, the temperature drops to 355-372 K, confirming that proper airflow management enables effective temperature regulation throughout the system.

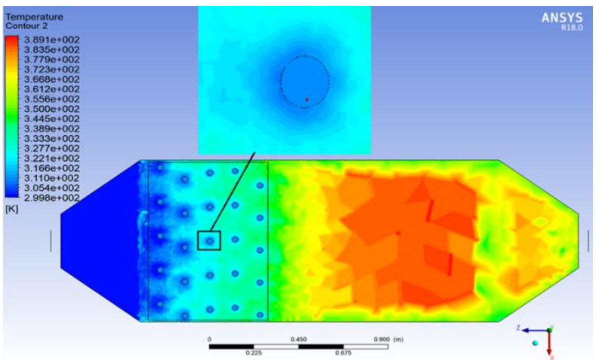

Figure 7. Temperature distribution of the collector during charging mode

Figure 8 displays the simulated temperature profile on the rear surface of the PV panel during the Nano-PCM charging process. The areas surrounding the Nano-PCM-filled tubes show notably lower temperatures, measured between 316-322 K. This observation reveals an important point: even though the PCM tubes do not cover the entire backside of the panel, their strategic placement successfully absorbs a considerable amount of excess heat from the panel, preventing overheating in the covered sections. This localized cooling effect offers multiple benefits. It helps maintain the PV panel at lower operating temperatures, which directly enhances its electrical output. At the same time, the absorbed thermal energy is stored within the Nano-PCM during its phase change.

This dual action not only improves panel performance but also contributes to extending its operational lifetime. Meanwhile, the panel sections without direct PCM tube contact follow a different thermal path. These areas transfer their heat to the collector plate beneath, causing temperatures to rise in those regions. On the temperature contour, these warmer zones appear in green and yellow. This creates a secondary heat transfer route within the system, in which excess heat from uncovered panel areas is transferred to the collector surface and then to the passing airflow.

The interaction between these two heat management paths, directing heat storage in the PCM and indirect heat transfer through the collector, highlights the effectiveness of the collector design. This thoughtful geometric arrangement proves highly suitable for hybrid photovoltaic-thermal (PV/T) systems, offering both stable performance and improved overall efficiency.

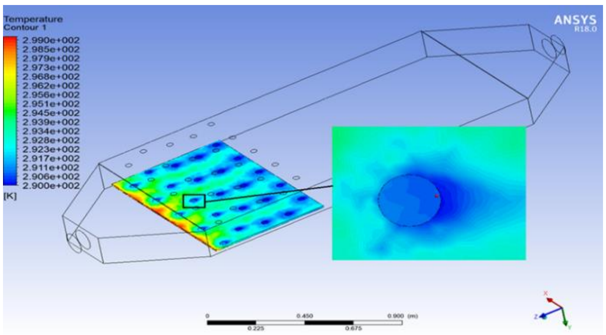

Figure 8. Temperature distribution on the PV panel backside during charging mode

3.2. Discharging Mode

Figure 9 presents the temperature contour from numerical simulations during the discharge phase. The results demonstrate that the collector's geometric design enables a controlled and gradual release of thermal energy previously stored in the Nano-PCM. The temperature distribution clearly shows the tubes containing Nano-PCM actively warming the passing airflow as they release their stored heat. The areas surrounding these tubes maintain moderate temperatures of 312-325 K, confirming effective heat transfer from the PCM to the air stream. An interesting pattern emerges when examining the collector plate surface. The central region displays elevated temperatures reaching 340-345 K, shown in red in the figure.

However, the outlet air temperature remains notably lower than this surface temperature. This temperature gap indicates that some thermal energy remains on the collector surface without being fully captured by the airflow. The primary reason for this incomplete heat transfer relates to air velocity and the limited time air spends inside the collector simply put, the air moves too quickly to absorb all available heat. Despite this limitation, the system design offers practical advantages.

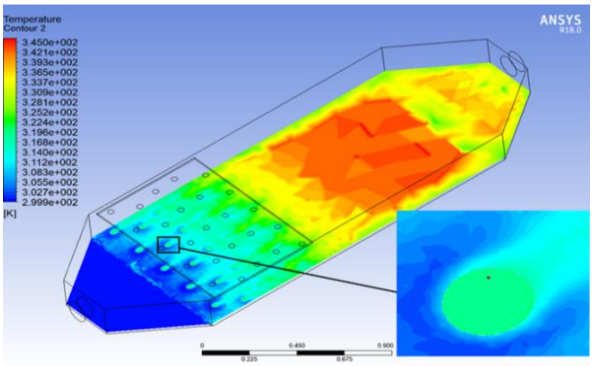

Figure 9. Temperature distribution of the collector during discharging mode

The outlet air temperature stays within a controllable and stable range, which helps maintain consistent thermal performance. This stability proves particularly valuable for applications sensitive to temperature fluctuations, such as drying medicinal plants, where sudden temperature changes could compromise product quality. The controlled discharge prevents excessive temperature spikes and maintains steady operating conditions throughout the process.

Figure 10 shows the simulation results for the photovoltaic panel. The back of the panel clearly shows the positive effect of using Nano-PCM during discharge. The temperature on the panel backside stays within a narrow and uniform range of 300 to 304 K. This means the PCM, by slowly releasing the stored heat, has kept the panel temperature at a good level and prevented local hotspots. The areas near the PCM-filled tubes show slightly higher temperatures. This indicates effective and continuous heat exchange between the phase change material and the panel surface. From a scientific perspective, these results suggest that using PCM not only improves the thermal performance of solar panels and increases their efficiency, but also reduces thermal stress and extends their lifetime.

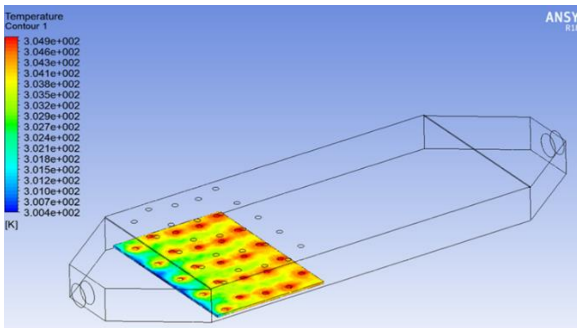

Figure 10. Temperature distribution on the PV panel backside during discharging mode

3.3. Velocity contours

The fluid enters the collector at an inlet velocity of 1.0 m/s (indicated by the red region at the entrance) and flows through the array of copper tubes filled with paraffin before exiting from the opposite side. As illustrated in figure 11, upon reaching the tube bank region, the fluid encounters flow obstacles and a reduced effective cross-sectional area, causing its velocity to decrease to approximately 0.290 m/s, as shown by the light blue coloring. This velocity reduction improves thermal performance by increasing the fluid's residence time in contact with the paraffin-filled tubes, thereby enhancing heat transfer. After passing through the tube array and exiting the densely packed region, the flow gradually redevelops.

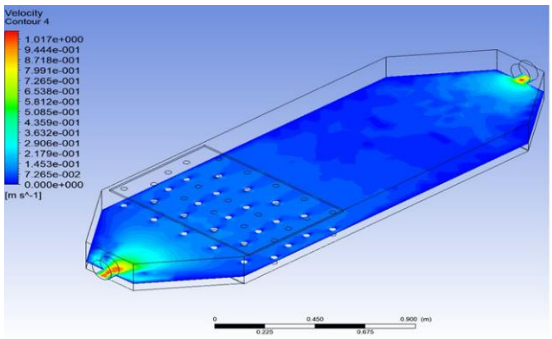

Figure 11. Contours of air velocity in the solar collector

4. Conclusions

In recent years, improving the efficiency of photovoltaic-thermal (PV/T) systems through thermal energy storage has attracted significant attention. This study evaluates the thermal performance of a PV/T collector integrated with copper tubes filled with nano-enhanced phase change material (nano-PCM), composed of paraffin wax doped with 3 %wt. zirconium oxide (ZrO_2) nanoparticles. Three-dimensional transient simulations were conducted using ANSYS Fluent to analyze heat transfer during charging and discharging cycles. The nano-PCM effectively moderated temperature variations across the collector surface, with peak temperatures reaching 389 K during charging and stabilizing at 345 K during discharging.

This thermal buffering capability promoted uniform heat distribution, reduced thermal stress on the PV panel, and enhanced overall system stability. The results confirm that nano-PCM integration significantly improves thermal regulation in PV/T collectors, making this configuration particularly suitable for applications requiring continuous thermal supply, such as solar dryers and hybrid renewable energy systems.

References:

Abdelrazik, A. S., Al-Sulaiman, F. A., Saidur, R., & Ben-Mansour, R. (2018). A review on recent development for the design and packaging of hybrid photovoltaic/thermal (PV/T) solar systems. Renewable and Sustainable Energy Reviews, 95, 110. https://doi.org/10.1016/j.rser.2018.07.024

Ahmadi, M., Arabhosseini, A., & Samimi-Akhijahani, H. (2025). Design and investigating the performance of the flat plate collector with photovoltaic panel and phase change material. Biomechanism and Bioenergy Research, 4(1), 32–43. https://doi.org/10.22103/bbr.2025.24483.110

Ahmadi, M., Samimi-Akhijahani, H., & Salami, P. (2023). Thermo-economic and drying kinetic analysis of oleaster using a solar dryer integrated with phase change materials and recirculation system. Journal of Energy Storage, 68, 107351. https://doi.org/10.1016/j.est.2023.107351

Arabhosseini, A. (2023). Application of clean energies in agricultural greenhouses. In Proceedings of the 8th International Conference on Technology and Energy Management (ICTEM). https://doi.org/10.1109/ICTEM56862.2023.10084219

Boyle, A. E., & Redgwell, C. (2021). Birnie, Boyle, and Redgwell's international law and the environment. Oxford University Press.

El-Afifi, M. I. (2024). Solar energy: Our future for sustainable energy. Nile Journal of Communication & Computer Science, 7(1), 67–83. https://doi.org/10.21608/njccs.2024.276627.1031

Hossain, M. F. (2021). Estimation of global solar energy to mitigate world energy and environmental vulnerability. In Renewable energy for mitigating climate change (1st ed., p. 28). CRC Press. https://doi.org/10.1201/9781003240120

Kaushik, E., Prakash, V., Mahela, O. P., Khan, B., El-Shahat, A., & Abdelaziz, A. Y.

(2022). Comprehensive overview of power system flexibility during the scenario of high penetration of renewable energy in utility grid. Energies, 15, 516. https://doi.org/10.3390/en15020516

Khoja, M. (2022). Solar energy applications for agriculture: A review. iManager's Journal on Power Systems Engineering, 10(3), 25. https://doi.org/10.26634/jps.10.3.19031

Koohi-Fayegh, S., & Rosen, M. A. (2020). A review of renewable energy options, applications, facilitating technologies and recent developments. *European Journal of Sustainable Development Research*, 4(4), em0138. https://doi.org/10.29333/ejosdr/7900

Kumar, C. M. S., Singh, S., Gupta, M. K., Nimdeo, Y. M., Raushan, R., Deorankar, A. V., et al. (2023). Solar energy: A promising renewable source for meeting energy demand in Indian agriculture applications. Sustainable Energy Technologies and Assessments, 55, 102905. https://doi.org/10.1016/j.seta.2022.102905

Lämmle, M., Oliva, A., Hermann, M., Kramer, K., & Kramer, W. (2017). PVT collector technologies in solar thermal systems: A systematic assessment of electrical and thermal yields with the novel characteristic temperature approach. Solar Energy, 155, 867–879. https://doi.org/10.1016/j.solener.2017.07.025

Mahdi, L. A., Chaichan, M. T., Abass, K. I., Fayad, M. A., Abdul-Wahab, H. A., & Kazem, H. A. 2024. Characterization of the thermophysical properties of paraffin-based nanocomposite containing alumina and iron oxide nanoparticles. In Advances in Material Science and Engineering. pp: 89–100. https://doi.org/10.1007/978-981-99-7389-5_10

Makieła, K., Mazur, B., & Głowacki, J. (2022). The impact of renewable energy supply on economic growth and productivity. Energies, 15, 4808. https://doi.org/10.3390/en15134808

Mishra, S. K., Gupta, M. K., Kumar, R., & Sharma, A. (2025). Performance enhancement of thermal energy storage system using ZrO_2 doped paraffin wax. Journal of Thermal Engineering, 11 (1), 79–93. https://doi.org/10.14744/thermal.0000905

Nandi, A., & Biswas, N. (2025). Melting dynamics and energy efficiency of nano-enhanced phase change material (NePCM) with graphene, Al_2O_3, and CuO for superior thermal energy storage (TES). *Journal of Energy Storage*, 109, 115076. https://doi.org/10.1016/j.est.2024.115076

Nair, D. R., Nair, M. G., & Thakur, T. (2022). A smart microgrid system with artificial intelligence for power-sharing and power quality improvement. Energies, 15, 5409. https://doi.org/10.3390/en15155409

Rezk, H., Alamri, B., Aly, M., Fathy, A., Olabi, A. G., Abdelkareem, M. A., & Ziedan, H. A. (2021). Multicriteria decision-making to determine the optimal energy management strategy of hybrid PV–diesel battery-based desalination system. Sustainability, 13, 4202. https://doi.org/10.3390/su13084202

Singh, S. N., Tiwari, P., & Tiwari, S. (Eds.). (2021). Fundamentals and innovations in solar energy: Energy systems in electrical engineering. Springer. https://doi.org/10.1007/978-981-33-6456-1

Sirin, C., Selimefendigil, F., & Öztop, H. F. (2023). Performance analysis and identification of an indirect photovoltaic thermal dryer with aluminum oxide nanoembedded thermal energy storage modification. Sustainability, 15, 2422. https://doi.org/10.3390/su15032422

Tay, N.H.S., Bruno, F. and Belusko, M. 2012. Experimental validation of a CFD model for tubes in a phase change thermal energy storage system. International Heat and Mass Transfer, 55: 574-585.

Zheng, X., & Zhou, Y. (2023). A three-dimensional unsteady numerical model on a novel aerogel-based PV/T-PCM system with dynamic heat-transfer mechanism and solar energy harvesting analysis. Applied Energy, 338, 120899. https://doi.org/10.1016/j.apenergy.2023.120899

Zhou, F., Ji, J., Yuan, W., Zhao, X., & Huang, S. (2019). Study on the PCM flat-plate solar collector system with antifreeze characteristics. International Journal of Heat and Mass Transfer, 129, 357–366. https://doi.org/10.1016/j.ijheatmasstransfer.2018.09.105